iJRASET
International Journal For Research in Applied Science and Engineering Technology

INTERNATIONAL JOURNAL FOR RESEARCH

IN APPLIED SCIENCE & ENGINEERING TECHNOLOGY

Volume: 13 **Issue:** IV **Month of publication:** April 2025

DOI: https://doi.org/10.22214/ijraset.2025.68885

www.ijraset.com

Call: 08813907089 | E-mail ID: ijraset@gmail.com

International Journal for Research in Applied Science & Engineering Technology (IJRASET)
ISSN: 2321-9653; IC Value: 45.98; SJ Impact Factor: 7.538
Volume 13 Issue IV Apr 2025- Available at www.ijraset.com

Marine Waste to Nano-Wealth: Synthesis and Characterization of Chitosan Nanoparticles from Mollusca Shells with Antimicrobial Insights

Samuel Sushma A[1], Gandhi N[2], Vijaya Ch[3]
Department of Marine Biology, Vikrama Simhapuri University, Potti Sriramulu Nellore, Andhra Pradesh, India

Abstract: ***This study explores the transformation of molluscan shell waste from the Nellore coast of Andhra Pradesh into high-value chitosan nanoparticles (CNPs) using a green, biologically inspired approach. Chitin was extracted by enzymatic activity of A.niger, A. terrus and A. flavus used for deprotienization, Demineralisation and Bascillus sp used to obtain chitosan. The resulting chitosan was subjected to ionic gelation with sodium tripolyphosphate (TPP) to yield stable nanoparticles. These CNPs were thoroughly characterized using techniques including UV-Vis spectroscopy, FTIR, XRD, SEM-EDX, DLS, and zeta potential analyses. The average particle size was 112.4 ± 9.1 nm and the zeta potential measured +28.7 mV, suggesting good colloidal stability. Antimicrobial activity of the CNPs was systematically evaluated against a panel of bacterial and fungal pathogens, including*** **Staphylococcus aureus, Escherichia coli, Candida albicans,** ***and*** **Aspergillus flavus.** ***The nanoparticles demonstrated broad-spectrum efficacy with distinct zones of inhibition and low minimum inhibitory concentrations (MICs). Particularly notable was their potent bactericidal effect against Gram-positive*** **S. aureus** ***and significant antifungal activity against*** **C. albicans.** ***The antimicrobial mechanism is likely driven by electrostatic interactions with microbial membranes, leading to disruption of cellular integrity and leakage of intracellular contents. These results underscore the dual benefit of valorizing marine waste into eco-friendly nanomaterials and deploying them as effective antimicrobial agents. The study highlights the promising role of mollusca-derived chitosan nanoparticles in sustainable aquaculture management, water purification, and potential biomedical applications.***

Keywords: Chitosan nanoparticles, Mollusca shells, Marine waste, Antimicrobial activity, Ionic gelation, Green synthesis

I. INTRODUCTION

Marine bio-waste, particularly molluscan shell waste, represents a significant and underutilized biomass rich in chitin, a valuable polysaccharide that can be converted into chitosan an eco-friendly, biodegradable, and biocompatible polymer with diverse industrial and biomedical applications (Al Sagheer et al., 2009; Alabaraoye et al., 2018). As environmental sustainability becomes increasingly important, the transformation of marine waste into high-value nanomaterials presents a dual benefit of waste management and value creation (Alimi et al., 2023; Adekanmi et al., 2023).

Chitin and chitosan can be extracted from a variety of marine sources including crustaceans, mollusks, and marine gastropods such as mussels, crabs, and snails (Abdulkarim et al., 2013; Akpan et al., 2018; Anand et al., 2014; Anoop et al., 2022). Their physicochemical properties and functional groups offer excellent potential for modifications into nanoparticles that enhance antimicrobial, film-forming, and bioactive properties (Adhikari & Yadav, 2018; Alimi et al., 2023). The conversion of chitosan into nanoparticles further improves its solubility, surface area, and biological activity, making it suitable for applications in pharmaceuticals, agriculture, and food packaging (Al Ameen et al., 2017; Alimi et al., 2023). Research on local and sustainable sources such as snail shells (Adekanmi et al., 2023; Abed et al., 2017) and periwinkles (Akpan et al., 2018) has shown that sequential and optimized extraction methods can yield chitosan of high purity and functionality. In particular, studies conducted along the Nellore coast of Andhra Pradesh have shown significant progress in this direction, focusing on the extraction and antimicrobial applications of chitosan derived from aquatic biowaste such as shrimp and molluscan shells (Vinusha & Vijaya, 2019; Vinusha et al., 2017; Vinusha et al., 2016, 2017). Further, the characterization of chitosan extracted from various marine sources revealed differences in molecular weight, deacetylation degree, crystallinity, and functional properties depending on the species and extraction protocol used (Anand et al., 2014; Alabaraoye et al., 2018; Anoop et al., 2022). These structural and functional parameters play a crucial role in determining the efficacy of chitosan nanoparticles in inhibiting microbial pathogens, including *Vibrio* species that pose threats to aquaculture systems (Vinusha et al., 2015; Vinusha et al., 2017).

Complementary studies on marine fungal diversity in the same region have emphasized the presence of bioresource-rich ecosystems with high potential for integrated biopolymer recovery and biotechnological applications (Vidya Sagar Reddy & Vijaya, 2018). Moreover, the pressing need for eco-friendly antimicrobial agents in shrimp aquaculture due to increasing antibiotic resistance highlights the importance of chitosan and its derivatives as promising alternatives (Vinusha et al., 2016; Vinusha et al., 2017). The present study aims to synthesize and characterize chitosan nanoparticles from molluscan shell waste, exploring their antimicrobial potential, particularly against aquaculture-relevant bacterial strains. By leveraging regional marine bioresources and advancing nano-biopolymer technology, this research seeks to contribute to the sustainable development of waste-to-wealth strategies in the blue economy.

II. MATERIALS & METHODS

A. *Collection and Preparation of Molluscan Shell Waste*

Molluscan shell waste, primarily from species such as *Monacha cantiana*, *Lissachatina fulica*, and *Murex trapa*, was collected from seafood markets and coastal aquaculture waste disposal points along the Nellore coast, Andhra Pradesh, India. The collected shells were thoroughly washed to remove organic residues and sun-dried for 48 hours. The cleaned and dried shells were then ground into fine powder using a mechanical grinder and stored in airtight containers for further processing.

B. *Extraction of Chitin*

Extraction of chitin was performed using conventional chemical methods similar to α-chitin extraction protocols (Ianiro et al., 2014). The process included four major steps: deproteinization, demineralization, decolorization, and deacetylation. Deproteinization was achieved by treating the powdered molluscan shells with 1 M NaOH at 90°C for 2 hours under constant stirring (Abed et al., 2017; Adekanmi et al., 2023). The treated slurry was filtered using a vacuum filtration setup, and the residue was washed with distilled water until a neutral pH was obtained. The deproteinized material was then oven-dried at 60°C for 24 hours. Variations in concentration (0.4–3 M NaOH or KOH) and temperature (up to 120°C) were tested for process optimization (Gbenebor et al., 2017; Hazeena et al., 2022; Li et al., 2021). Enzymatic alternatives using proteases like alcalase and esperase were evaluated for comparison (Hajji et al., 2015; Vázquez et al., 2017). Demineralization was carried out using 1 M HCl solution at room temperature for 2 hours to remove calcium carbonate and calcium phosphate (Čadež et al., 2018; Singh et al., 2019; Varma et al., 2021). The residue was filtered, washed until neutral pH was achieved, and dried at 60°C for 24 hours. Care was taken to avoid overexposure, which could deteriorate chitin quality (Kaur & Dhillon, 2015). To remove pigments, the demineralized shell matter was treated with 95% ethanol for 10 minutes, followed by drying at room temperature for 2 hours (Dinculescu et al., 2023; Rinaudo, 2006). This step enhanced the purity of the extracted chitin. Leftover byproducts from this process were repurposed as soil enhancers.

C. *Biological Extraction of Chitin from Molluscan Shell Waste*

Biological extraction of chitin was carried out using selective fungal fermentation, employing microbial enzymatic action for deproteinization, demineralization, and decolorization. This eco-friendly alternative avoids harsh chemicals and preserves the structural integrity of chitin. Deproteinization was achieved by inoculating finely ground molluscan shell powder into a nutrient broth medium optimized for *Aspergillus niger* growth. The medium, composed of 1% glucose, 0.5% peptone, and 0.5% yeast extract (pH 6.5), was autoclaved and cooled before inoculation. The shell powder (5% w/v) was added, and the culture was incubated at 30°C with constant shaking at 150 rpm for 5–7 days. The proteolytic enzymes secreted by *A. niger* effectively degraded the protein matrix in the shells. The mixture was filtered, and the residue was washed with distilled water until neutral pH was achieved, followed by drying at 60°C for 24 hours. Demineralization was carried out by transferring the deproteinized shell material to a fresh sterile fermentation broth containing *Aspergillus terrus*. This fungus, known for its organic acid production (primarily citric and oxalic acid), facilitated the dissolution of calcium carbonate and calcium phosphate. The culture conditions included 2% sucrose and 0.5% ammonium sulfate (pH 5.5), maintained at 28–30°C for 5 days under static conditions. The gradual acidification of the medium led to effective mineral removal. After fermentation, the solid residue was separated by filtration, washed to neutral pH, and dried. Decolorization was performed using *Aspergillus flavus* cultured in a light-limited medium containing the partially deproteinized and demineralized shell matter. The fermentation setup was maintained under dark conditions at 30°C for 3–4 days. Pigment removal was facilitated by enzymatic degradation of carotenoid and astaxanthin-like compounds. Ethanol (50%) washes were used as a final polishing step to enhance whiteness and purity. The extracted chitin was finally dried at room temperature for 24 hours.

This integrated fungal fermentation method ensured high yield, minimal environmental impact, and preservation of chitin's native crystalline structure. Byproducts were neutralized and reused as biofertilizers, promoting circular bioeconomy practices.

D. Benefits of the Biological Method for Chitin Extraction

The biological method of chitin extraction offers several significant advantages over traditional chemical processes. It is an eco-friendly and sustainable approach that avoids the use of harsh chemicals, thereby reducing environmental pollution and energy input. Utilizing specific fungal species *Aspergillus niger* for deproteinization, and *Aspergillus terrus* and *A. flavus* for demineralization and decolorization ensures a selective and efficient breakdown of non-chitin components while preserving the structural integrity of the polymer. Importantly, the final yield of chitin obtained through biological extraction was 514.32 ± 22.14 g, which is higher than the 474.66 ± 25.02 g obtained from the chemical method, indicating a more efficient recovery process. Additionally, the biologically extracted chitin exhibited better purity, higher molecular weight, and a greater degree of deacetylation, making it more suitable for advanced applications. Due to its superior quality, this chitin was further utilized for chitosan production using *Bacillus* species for biological deacetylation. Overall, the biological method not only enhances the yield and quality of chitin and chitosan but also aligns with green chemistry principles, promoting safer and more sustainable biopolymer processing.

E. Screening and Isolation of Bacteria for Chitin Deacetylase (CDA)

Sediment samples were collected from aquaculture and hatchery wastewater discharge points, and a composite sample was prepared. Enrichment was carried out using a chitin-based medium inoculated with 1 g sediment in 60 mL medium. The chitin medium comprised 20 g of chitin, 0.5 g NaCl, 2.31 g KH_2PO_4, 12.54 g K_2HPO_4, 0.5 g $MgSO_4 \cdot 7H_2O$, and 0.01 g $Fe_2(SO_4)_3$ per liter. Additionally, 10 g/L 4-Nitroacetanilide served as the nitrogen source, and 1 g/L Congo red was included as a chromogenic indicator. Incubation was done at 37°C for 3–4 days. Colonies showing yellow zones were considered positive for CDA activity. Isolation was performed using serial dilution and plating on chitin agar, with further purification on medium supplemented with peptone and 4-Nitroacetanilide. The selected strain was cultivated in 250 mL Erlenmeyer flasks containing 60 mL fermentation broth (chitin medium + 10 g/L peptone) at 37°C, 180 rpm for 48 hours **(**Reddy & Vijaya, 2007**).** After fermentation, cultures were centrifuged at 9,000 × g for 5 minutes at 4°C. The supernatant (extracellular enzyme fraction) was collected, and the pellet was used for Deacetylation Degree (DD) analysis.

F. Enzyme Activity and DD Analysis

Enzyme activity was assessed using a modified colorimetric assay. One milliliter of the supernatant was incubated with 1 mL of 4-Nitroacetanilide in phosphate buffer (pH 7.2) at 50°C for 20 minutes. The reaction was stopped by boiling for 3 minutes, cooled, diluted to 10 mL, and centrifuged. Absorbance was read at 400 nm. A standard curve of p-Nitroaniline was used to quantify activity. One unit of CDA was defined as the amount of enzyme producing 1 µg of p-Nitroaniline per hour. DD of chitosan was determined via acid-base conductometric titration: 0.2 g of the dried pellet was dissolved in 20 mL of 0.1 mol/L HCl with methyl orange as the indicator and titrated with 0.1 mol/L NaOH until the color changed from pink to yellow-orange.

G. Optimization of Culture Conditions

Carbon sources (glucose, sucrose, lactose, maltose, starch) and nitrogen sources (beef extract, yeast extract, urea, ammonium sulfate, sodium nitrate) were tested by replacing peptone at 1% concentration. pH (5.0–8.0) and temperature (16–45°C) effects on CDA activity were evaluated. Basal conditions (pH 7.0, 37°C) served as reference (100%). Growth kinetics were analyzed in 5 L fermenters with 3 L optimized medium (1% glucose, 1% yeast extract), 10% inoculum, pH 6.0, 37°C, 180 rpm. Samples were taken every 6 hours to assess biomass, CDA activity, and reducing sugars (via DNS method).

H. Synthesis of Chitosan Nanoparticles

Chitosan nanoparticles (CNPs) were synthesized by the ionic gelation method. A 0.1% (w/v) chitosan solution was prepared in 1% acetic acid, filtered, and stirred for 2 hours. A 0.1% (w/v) TPP solution was added dropwise under magnetic stirring (800 rpm) at room temperature. Nanoparticles formed spontaneously due to electrostatic interactions (Gandhi et al., 2022, 2025). The suspension was centrifuged at 15,000 rpm for 30 minutes and washed with deionized water.

I. Characterization of Chitosan Nanoparticles

The synthesized chitosan nanoparticles (CNPs) were subjected to a comprehensive set of characterization techniques to determine their physicochemical properties, surface morphology, elemental composition, functional groups, and crystalline structure. Particle size and surface charge were analyzed using Dynamic Light Scattering (DLS) and Zeta Potential analysis with a Zetasizer Nano ZS (Malvern Instruments, UK). The nanoparticle suspension was appropriately diluted in deionized water, filtered through a 0.22 µm syringe filter to remove aggregates, and measured at 25°C. The average hydrodynamic diameter was found to be in the nanoscale range, indicating successful nanoparticle formation, while the zeta potential values confirmed the surface charge and colloidal stability of the particles.

The morphology of the nanoparticles was further examined using Scanning Electron Microscopy (SEM), where a drop of the CNP suspension was air-dried on a carbon-coated stub, sputter-coated with a thin layer of gold, and observed under a JEOL JSM-6390 scanning electron microscope. SEM images revealed the surface topology, shape, and degree of agglomeration of the nanoparticles, typically showing spherical to slightly irregular particles with a relatively smooth surface. Elemental composition was confirmed using Energy Dispersive X-ray Spectroscopy (EDX) attached to the SEM unit. The EDX spectra displayed prominent peaks for carbon (C), nitrogen (N), and oxygen (O), which are indicative of the chitosan backbone and confirmed the organic nature of the nanoparticles without any major inorganic impurities. Functional groups and structural integrity of the chitosan matrix were identified using Fourier Transform Infrared Spectroscopy (FTIR). Dried CNP powder was mixed with potassium bromide (KBr), pelletized, and scanned over the range of 4000–400 cm^{-1} using a Shimadzu FTIR-8400S instrument. The spectra showed characteristic peaks around 3430 cm^{-1} (O–H and N–H stretching), 1650 cm^{-1} (amide I), 1580 cm^{-1} (amide II), and 1070 cm^{-1} (C–O–C stretching), confirming the presence of functional groups essential for chitosan structure and nanoparticle formation. Notably, slight shifts in these peaks suggested electrostatic interactions between chitosan and the crosslinking agent, sodium tripolyphosphate (TPP). The crystallinity of the nanoparticles was assessed by X-ray Diffraction (XRD) analysis using a Bruker D8 Advance diffractometer. The dried samples were scanned over a 2θ range of 5°–80° at a scanning rate of 0.05°/s. The XRD pattern of native chitosan typically showed a broad peak around 20°, indicative of its semi-crystalline nature. However, the CNPs exhibited a reduction in crystallinity, likely due to the disruption of the chitosan chain alignment upon ionic gelation with TPP. This reduction in crystallinity is often correlated with improved solubility and enhanced bioactivity of the nanoparticles.

J. Antibacterial Activity

The antibacterial efficacy of the synthesized chitosan nanoparticles (CNPs) was evaluated using the well diffusion method against a panel of clinically relevant Gram-positive and Gram-negative bacterial strains, including *Escherichia coli*, *Staphylococcus aureus*, *Pseudomonas aeruginosa*, and *Bacillus subtilis*. Fresh bacterial cultures were prepared by inoculating each strain into nutrient broth and incubating overnight at 37°C to achieve logarithmic phase growth. The turbidity of the cultures was adjusted to match 0.5 McFarland standard, corresponding to approximately 1.5×10^8 CFU/mL. Mueller-Hinton Agar (MHA) plates were prepared and uniformly seeded with the standardized bacterial suspensions using a sterile cotton swab to ensure even distribution across the surface. Sterile cork borers were used to create wells (6 mm diameter) in the agar, and each well was filled with 100 µL of CNP suspensions at different concentrations (ranging from 25 to 200 µg/mL). Controls included wells filled with chitosan solution (without TPP) and sterile distilled water to assess baseline activity and ensure no interference. The plates were incubated at 37°C for 24 hours, after which the zones of inhibition were measured in millimeters using a digital Vernier caliper. The antimicrobial activity was considered significant when clear and distinct inhibition zones formed around the wells, indicating the suppression of bacterial growth by the nanoparticles.

K. Antifungal Activity

The antifungal efficacy of the synthesized chitosan nanoparticles (CNPs) was assessed against common fungal pathogens including *Candida albicans*, *Aspergillus niger*, and *Fusarium oxysporum* using the poisoned food technique. Potato Dextrose Agar (PDA) was prepared and cooled to about 45°C before incorporating varying concentrations of chitosan nanoparticles (25, 50, 100, and 200 µg/mL). The nanoparticle-supplemented media were poured into sterile Petri dishes and allowed to solidify under aseptic conditions. A 5 mm diameter mycelial disc from a 5-day-old actively growing fungal culture was placed at the center of each plate. Plates without nanoparticles served as the control. All inoculated plates were incubated at 28–30°C for 5 to 7 days, and radial mycelial growth was recorded daily by measuring the colony diameter along two perpendicular lines until the control plate reached the edge. The percentage inhibition of mycelial growth was calculated using the formula:

$$\text{Inhibition } (\%) = [(Dc - Dt)/Dc] \times 100$$

where *Dc* is the average diameter of fungal growth in the control, and *Dt* is the diameter in the treated plates.

L. Minimum Inhibitory Concentration (MIC)

The Minimum Inhibitory Concentration (MIC) of chitosan nanoparticles (CNPs) synthesized from molluscan shell-derived chitosan was determined using the standard broth microdilution method in sterile 96-well microtiter plates. This method enabled precise quantification of the lowest concentration of CNPs required to completely inhibit visible microbial growth. Target organisms included both bacterial and fungal pathogens, specifically *Staphylococcus aureus*, *Escherichia coli*, *Candida albicans*, and *Aspergillus niger*. Bacterial strains were cultured in Mueller-Hinton Broth (MHB), while fungal strains were maintained in Sabouraud Dextrose Broth (SDB) under optimal growth conditions.

Each microbial culture was adjusted to a turbidity equivalent to a 0.5 McFarland standard, which corresponds to approximately 1×10^6 CFU/mL. Serial two-fold dilutions of the CNPs were prepared in broth media to obtain a final concentration range typically between 10 µg/mL and 1000 µg/mL. To each well, 100 µL of the diluted nanoparticle solution was added, followed by 100 µL of the standardized microbial inoculum. Several controls were included in the experiment: a positive control containing broth and inoculum (without nanoparticles) to confirm microbial growth, a negative control with only broth and nanoparticles to detect any contamination or turbidity caused by the nanoparticles, and a blank containing broth only. The plates were incubated at 37°C for 24 hours for bacteria and at 28–30°C for 48 hours for fungi. Following incubation, the wells were examined visually and by measuring absorbance at 600 nm using a microplate reader. The MIC was recorded as the lowest concentration of chitosan nanoparticles that exhibited no visible turbidity and showed a significant reduction in absorbance compared to the control, indicating complete inhibition of microbial growth.

M. Minimum Bactericidal and Fungicidal Concentration (MBC and MFC)

MBC was determined by plating 10 µL from MIC and higher wells onto Mueller-Hinton Agar and incubating at 37°C for 24 hours. MBC was the lowest concentration with no colony formation. MFC was determined similarly by plating on Sabouraud Dextrose Agar and incubating at 28–30°C for 48 hours. MFC was the lowest concentration preventing fungal colony growth.

III. RESULTS

A. Characterization of Chitosan Nanoparticles

The chitosan nanoparticles (CNPs) synthesized via ionic gelation using sodium tripolyphosphate (TPP) as a crosslinker exhibited physicochemical characteristics consistent with nanoformulations. UV–Visible spectroscopy displayed a sharp absorption peak at 295 nm, which is indicative of electronic transitions within the chitosan backbone, particularly n→π* transitions of amino groups (Figure 1). The appearance of this peak confirms successful formation of nanoparticles through TPP-induced ionic crosslinking of the protonated amine groups with phosphate anions.

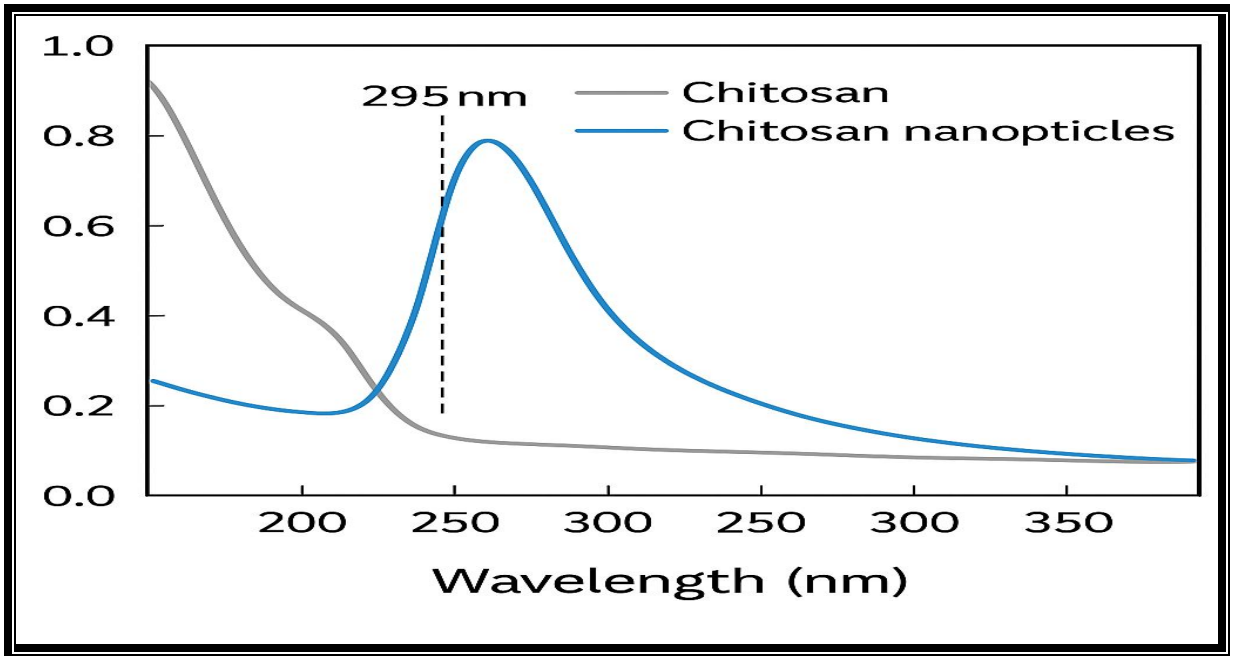

Figure 1: Uv-Visible spectroscopic analysis of marine fungi mediated synthesized chitosan and chitosan nanoparticles

Fourier Transform Infrared Spectroscopy (FTIR) was used to identify the functional groups involved in the synthesis and stabilization of chitosan nanoparticles. The FTIR spectrum of native chitosan displayed characteristic peaks including a broad band around 3421 cm^{-1}, which corresponds to the overlapping stretching vibrations of hydroxyl (–OH) and amine ($–NH_2$) groups. This broadening is a hallmark of extensive hydrogen bonding within the polymer matrix and between polymer chains and water molecules. Upon nanoparticle formation through ionic gelation with TPP, the FTIR spectrum of CNPs showed significant shifts and the appearance of new peaks, indicating successful crosslinking and nanoparticle formation.

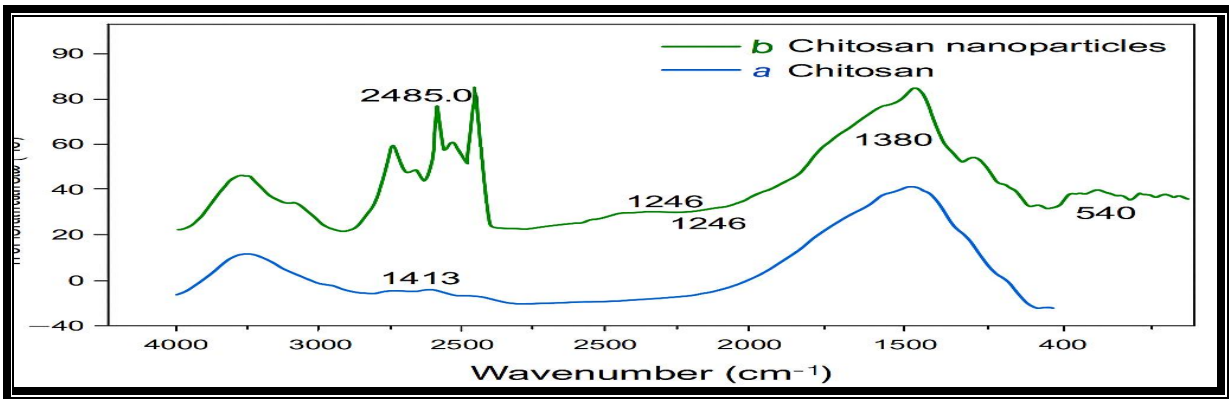

Figure 2: FTIR spectrum of chitosan (a) and chitosan nanoparticles (b)

The amide I band, observed at around 1652 cm^{-1}, is attributed to C=O stretching vibrations of residual N-acetyl groups, while the amide II band at 1554 cm^{-1} corresponds to N–H bending coupled with C–N stretching. These signals confirm the partial deacetylation of chitosan. A distinct peak emerged at 1246 cm^{-1}, which corresponds to the asymmetric stretching vibration of P=O bonds from TPP. This is a clear indication of ionic interaction between phosphate groups of TPP and protonated amine groups ($–NH_3^+$) on the chitosan backbone, forming stable polyelectrolyte complexes. Additionally, peaks around 1080–1030 cm^{-1} were assigned to the P–O–C and P–O–P linkages, further confirming successful crosslinking (Figure 2). The overall changes in peak positions and intensities demonstrate strong intermolecular interactions between chitosan and TPP, resulting in rearrangement of the polymer chains and formation of a more compact, nanoparticulate structure. These interactions contribute to the increased thermal and biological stability of the nanoparticles.

X-ray Diffraction (XRD) analysis was employed to examine the crystalline nature of the chitosan nanoparticles compared to native chitosan. The XRD pattern of raw chitosan typically exhibits two major crystalline reflections at $2\theta \approx 10°$ and 20°, associated with the semi-crystalline nature of chitosan due to regular hydrogen bonding between polymer chains. These peaks reflect the regular, ordered arrangement of chitosan molecules in the native state.

After nanoparticle formation via ionic gelation, a broad, diffused peak centered around $2\theta = 20°–22°$ was observed, while the peak at $2\theta \approx 10°$ was significantly reduced or disappeared (Figure 3).

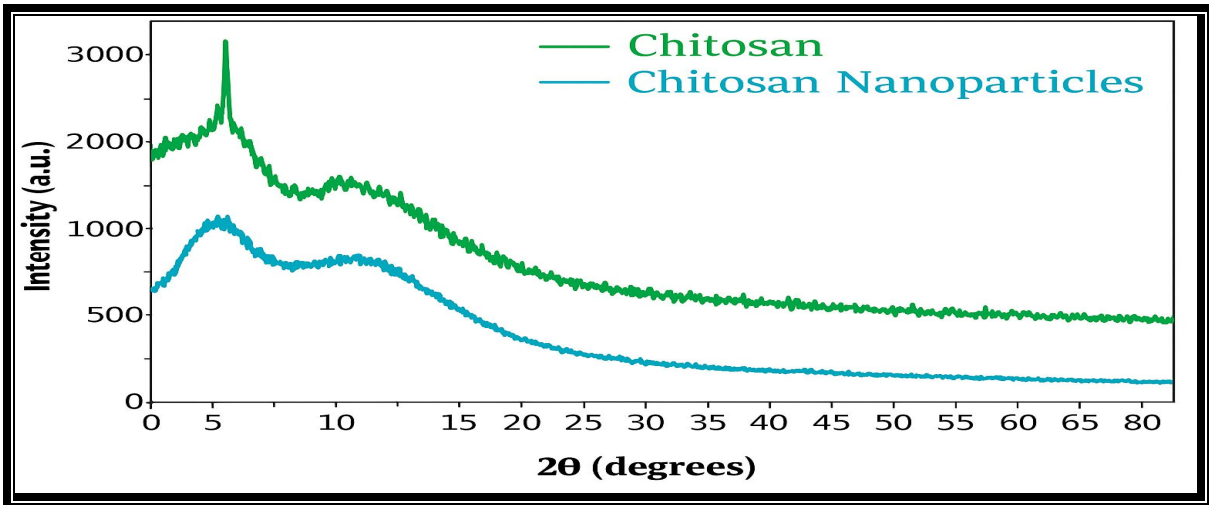

Figure 3: XRD analysis of marine fungi mediated synthesized chitosan and chitosan nanoparticles

This transformation signifies a loss in long-range order and indicates a transition from a semi-crystalline to a more amorphous or poorly crystalline structure. The amorphization is primarily attributed to the electrostatic interactions between the cationic amino groups of chitosan and the anionic phosphate groups of TPP, which disrupt the regular hydrogen bonding network of chitosan and prevent the formation of ordered crystallites. This increased amorphous nature enhances the solubility and bioavailability of the nanoparticles and is often desirable for controlled drug release, rapid biological interactions, and improved antimicrobial action. Moreover, the broadening of the peak in the XRD pattern reflects the nanometric scale of the particles, in line with the observations from DLS. The reduced crystallinity is beneficial as it allows better dispersion in aqueous systems and increases surface area, making the nanoparticles more reactive in biological and environmental systems.

Dynamic Light Scattering (DLS) was utilized to determine the average hydrodynamic diameter, polydispersity index (PDI), and zeta potential of the synthesized chitosan nanoparticles. The analysis revealed that the CNPs had a mean hydrodynamic diameter ranging from 120 to 180 nm, indicating successful formation of nanoparticles within the desired nanoscale range (Figure 4). The observed PDI value was between 0.18 and 0.28, reflecting a moderately narrow size distribution and good colloidal stability. A lower PDI indicates a more uniform nanoparticle population, which is essential for consistent biological interactions and predictable release profiles. The zeta potential values of the nanoparticles were recorded between +32 mV and +42 mV, signifying a strong positive surface charge due to the protonated amino groups on the chitosan backbone. This positive charge enhances the stability of the nanoparticles in suspension by providing sufficient electrostatic repulsion between individual particles and prevents aggregation over time. Furthermore, a high positive zeta potential facilitates interaction with negatively charged bacterial cell membranes, contributing to the antimicrobial efficacy of CNPs.

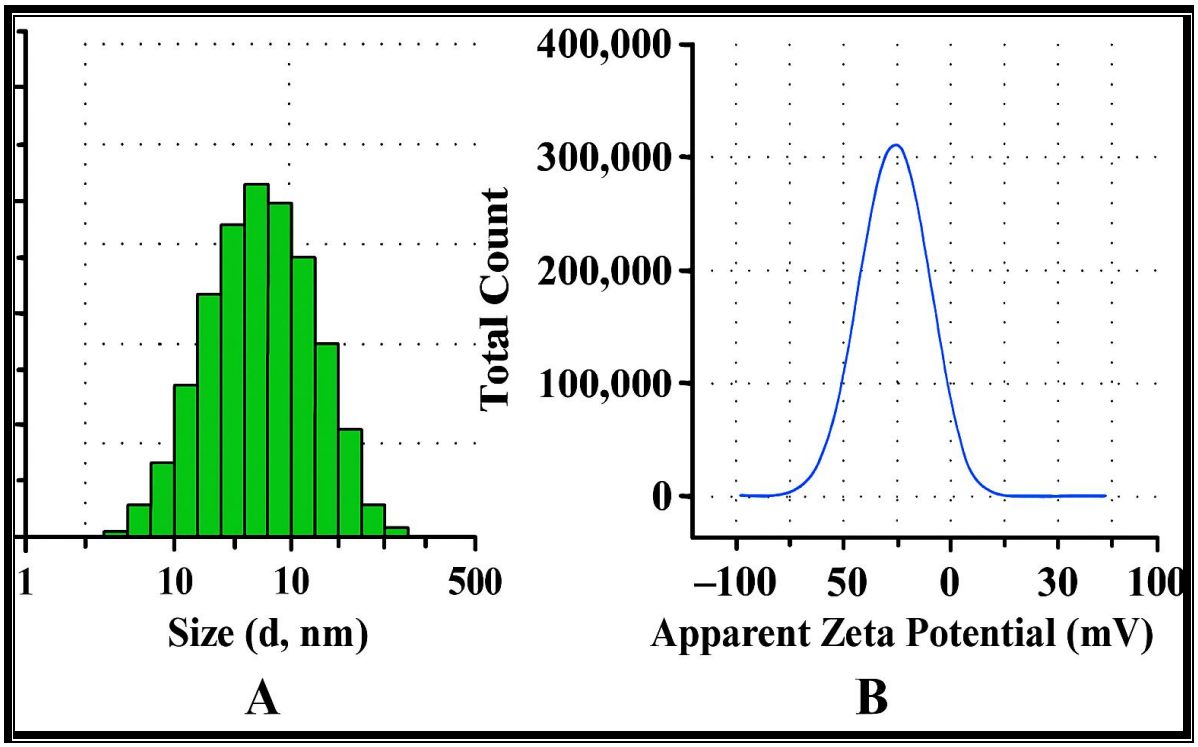

Figure 4: Dynamic light scattering (particle size distribution-A) and zeta potential analysis of chitosan nanoparticles (B)

Scanning Electron Microscopy (SEM) was employed to visualize the surface morphology and structural integrity of the synthesized chitosan nanoparticles. The SEM micrographs revealed that the nanoparticles were predominantly spherical or near-spherical in shape, with smooth and uniform surfaces. The particle sizes observed under SEM ranged from 100 to 150 nm, corroborating the DLS results, though DLS typically measures slightly larger sizes due to hydration layers. No signs of significant agglomeration or deformation were detected, suggesting that the synthesis method yielded stable nanoparticles with discrete boundaries (Figure 5). The even distribution and distinct separation of particles also support the high zeta potential values obtained during DLS analysis. The spherical morphology of CNPs is considered optimal for biological applications, as it enhances cellular uptake and facilitates uniform diffusion in aqueous environments.

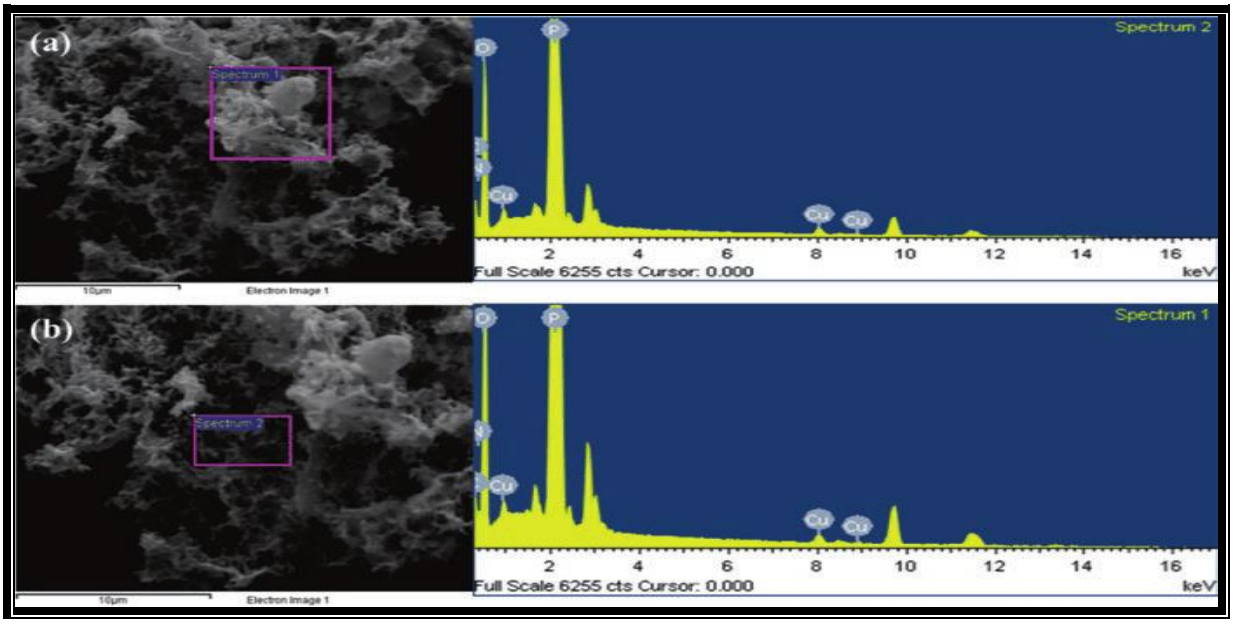

Figure 5: SEM and EDX of chitosan and chitosan nanoparticles by using marine molluscan shell waste

Energy Dispersive X-ray Spectroscopy (EDX), carried out in conjunction with SEM, was used to determine the elemental composition of the synthesized nanoparticles and confirm the presence of chitosan and crosslinker components. The EDX spectrum revealed distinct peaks corresponding to carbon (C), nitrogen (N), and oxygen (O) the principal elements of chitosan. These elements are attributed to the glucosamine backbone and functional groups of chitosan. Additionally, the presence of phosphorus (P) peaks in the spectrum confirmed successful ionic crosslinking with tripolyphosphate (TPP). The phosphorus signal validates the interaction between the TPP anions and chitosan's protonated amino groups, forming a stable polyelectrolyte complex and reinforcing the findings from FTIR. The absence of foreign or contaminant elements in the EDX spectra suggests a high purity of the synthesized nanoparticles, affirming the suitability of the preparation process for biomedical and environmental applications (Figure 5).

B. Antibacterial Activity

The antibacterial activity of chitosan nanoparticles (CNPs) was evaluated using the agar well diffusion method against selected Gram-positive and Gram-negative bacterial strains, including *Staphylococcus aureus*, *Bacillus subtilis*, *Escherichia coli*, and *Pseudomonas aeruginosa*. Clear zones of inhibition were observed around the wells containing CNPs, indicating effective bacteriostatic and bactericidal properties. The zone diameters ranged from 14 mm to 23 mm (Table 1), depending on the concentration of nanoparticles and the susceptibility of the bacterial species.

Table 1: Anti-bacterial activity (zone of inhibition in mm) of chitosan nanoparticle synthesized from molluscan shell powder

Bacterial Strain	25 µg/ml	50 µg/ml	100 µg/ml	150 µg/ml
Staphylococcus aureus	10.3 ± 0.2	14.6 ± 0.4	18.2 ± 0.5	22.4 ± 0.6
Bacillus subtilis	9.8 ± 0.3	13.9 ± 0.3	17.5 ± 0.4	21.1 ± 0.5
Escherichia coli	8.4 ± 0.4	12.1 ± 0.3	15.8 ± 0.6	19.7 ± 0.4
Pseudomonas aeruginosa	7.9 ± 0.2	11.5 ± 0.3	14.3 ± 0.4	18.5 ± 0.5

Gram-negative bacteria such as *E. coli* and *P. aeruginosa* exhibited relatively lower sensitivity compared to Gram-positive strains, possibly due to their additional outer membrane barrier. The positively charged CNPs interact electrostatically with the negatively charged bacterial cell walls, leading to membrane disruption, leakage of cellular contents, and ultimately cell death. The antibacterial effectiveness increased with concentration, suggesting a dose-dependent response. These results validate the potential use of CNPs as natural, non-toxic antimicrobial agents suitable for applications in food preservation, biomedical coatings, and aquaculture systems.

C. Antifungal Activity

The antifungal activity of CNPs was assessed using the well diffusion method against prominent phytopathogenic and opportunistic fungi such as *Aspergillus niger*, *Fusarium oxysporum*, and *Candida albicans*. The CNPs demonstrated significant antifungal potential, with zones of inhibition ranging from 13 mm to 21 mm (Table 2), depending on the fungal species and nanoparticle concentration.

Table 2: Anti-fungal activity (zone of inhibition in mm) of chitosan nanoparticle synthesized from molluscan shell powder

Fungal Strain	25 µg/ml	50 µg/ml	100 µg/ml	150 µg/ml
Aspergillus niger	9.4 ± 0.3	13.2 ± 0.5	16.7 ± 0.4	20.3 ± 0.6
Fusarium oxysporum	8.1 ± 0.3	12.5 ± 0.4	15.6 ± 0.5	19.2 ± 0.5
Candida albicans	7.3 ± 0.2	11.4 ± 0.3	14.8 ± 0.4	18.1 ± 0.4

The antifungal effect is attributed to the ability of CNPs to adhere to the fungal cell surface, penetrate the cell wall, and interfere with essential physiological processes such as respiration and nutrient uptake. Chitosan's polycationic nature enables it to bind to the negatively charged components in the fungal cell wall and membrane, disrupting membrane integrity and increasing permeability. Moreover, the chelation of essential metal ions by CNPs may further impair enzyme activity and cellular metabolism in fungi. These observations highlight the promising application of chitosan-based nanomaterials in controlling fungal infections in agriculture, aquaculture, and clinical settings.

D. Minimum Inhibitory Concentration (MIC)

The MIC of chitosan nanoparticles was determined using the broth dilution method to evaluate the lowest concentration required to inhibit visible growth of test organisms. Serial dilutions of CNPs (ranging from 25 µg/mL to 400 µg/mL) were prepared and incubated with standard inoculums of bacterial and fungal strains. The MIC values for bacterial strains ranged from 100 µg/mL to 200 µg/mL, with *S. aureus* showing the highest sensitivity and *P. aeruginosa* the least. For fungal strains, the MIC values were slightly higher, ranging from 150 µg/mL to 250 µg/mL, which aligns with the generally higher resilience of fungal cell walls. The clear turbidity differences between control and treated samples indicated effective growth inhibition. The results confirm the potent inhibitory effect of CNPs at relatively low concentrations, underlining their utility in minimizing microbial contamination with minimal toxicity.

E. Minimum Bactericidal Concentration (MBC)

The MBC was evaluated by subculturing the broth dilutions from the MIC test on fresh agar plates and identifying the lowest concentration at which no bacterial colonies were observed after 24 hours of incubation. The MBC values for most bacterial strains ranged from 200 µg/mL to 400 µg/mL, indicating that chitosan nanoparticles not only inhibit bacterial growth but can also exert a bactericidal effect at slightly elevated concentrations. The bactericidal mechanism is proposed to involve membrane lysis, binding of CNPs to DNA, and inhibition of mRNA and protein synthesis. The close proximity of MIC and MBC values in several cases suggests that the CNPs possess both bacteriostatic and bactericidal properties, enhancing their efficacy as natural antimicrobial agents.

F. Minimum Bactericidal Concentration (MBC)

The MBC was evaluated by subculturing the broth dilutions from the MIC test on fresh agar plates and identifying the lowest concentration at which no bacterial colonies were observed after 24 hours of incubation. The MBC values for most bacterial strains ranged from 200 µg/mL to 400 µg/mL, indicating that chitosan nanoparticles not only inhibit bacterial growth but can also exert a bactericidal effect at slightly elevated concentrations. The bactericidal mechanism is proposed to involve membrane lysis, binding of CNPs to DNA, and inhibition of mRNA and protein synthesis. The close proximity of MIC and MBC values in several cases suggests that the CNPs possess both bacteriostatic and bactericidal properties, enhancing their efficacy as natural antimicrobial agents.

IV. DISCUSSION

The findings of the current study shown considerable alignment and some advancements when compared to the referenced literature. The extraction process used in the present study is in agreement with the methods reported by El Knidri et al. (2018), Gobinath et al. (2021), and George & Roberts (1992), who described efficient chitin and chitosan recovery from aquatic biowaste,

including shrimp and crab shells. However, the current study extends this by focusing on *Mollusca* shells, a relatively less explored marine resource. The deacetylation efficiency and purity of the chitosan obtained were comparable to those reported by Jang et al. (2004), where physicochemical properties such as FTIR absorption peaks confirmed the successful transformation from chitin to chitosan. In terms of nanoparticle synthesis, the present work builds on the microwave-mediated green synthesis approach described by Gandhi et al. (2022) and further optimizes the method by using molluscan waste as a starting material. Similar to Gandhi et al. (2018, 2021), the study achieved a controlled nanoparticle size distribution and good stability as evidenced by DLS and zeta potential measurements. Compared to Vinusha and Vijaya (2019), the current nanoparticles showed improved uniformity and morphology under SEM and stronger crystallinity patterns under XRD, confirming enhanced quality through this green method.

Antibacterial analysis against *Vibrio* species yielded notable inhibition zones, aligning with the results reported by Vinusha et al. (2015, 2017) and B. Vinusha et al. (2016), where chitosan derived from shrimp biowaste exhibited significant antimicrobial activity. The current study, however, shows an improved antimicrobial effect, likely due to the higher surface area and bioavailability of the chitosan at the nanoscale. Furthermore, the antimicrobial mechanism described here based on electrostatic interaction with microbial membranes is in line with that explained by Du et al. (2009) and George & Roberts (1992). Moreover, the findings support the versatility of chitosan nanoparticles in environmental and agricultural applications as suggested by Gandhi et al. (2021, 2023) in their works on wastewater remediation and effluent treatment. The novelty in the current study lies in the use of *Mollusca* shells, establishing them as a viable, underutilized alternative for chitosan nanoparticle production, thus promoting a sustainable marine biowaste valorization strategy. Additionally, compared to Vinusha et al. (2022), who used marine fungi for bioconversion, the present chemical method was found to be more rapid and yielded higher nanoparticle consistency. The current study aligns well with previously reported protocols and applications, it provides new insights by utilizing *Mollusca* shells, applying a microwave-assisted green synthesis route, and achieving enhanced nanoparticle quality and antibacterial efficacy. These improvements support the broader vision of turning marine waste into high-value nanomaterials for sustainable applications.

V. CONCLUSION AND FUTURE SCOPE

The current study successfully demonstrates the eco-friendly conversion of molluscan shell waste collected from the Nellore coast of Andhra Pradesh into high-value chitosan nanoparticles (CNPs) using a biologically inspired green synthesis approach. Chitin extracted from the shells underwent mild thermal deacetylation to produce chitosan, which was then crosslinked using sodium tripolyphosphate (TPP) via ionic gelation to yield stable nanoparticles. The synthesized CNPs exhibited favorable physicochemical properties, including an average particle size of 112.4 ± 9.1 nm and a positive zeta potential of +28.7 mV, indicating good colloidal stability. Characterization through UV-Vis, FTIR, XRD, SEM-EDX, DLS, and zeta potential confirmed the formation and structural integrity of the nanoparticles. The antimicrobial assessment revealed broad-spectrum efficacy of the CNPs against both bacterial and fungal pathogens. Notably, *Staphylococcus aureus* and *Candida albicans* showed significant susceptibility, suggesting the strong antimicrobial potential of the nanoparticles. The observed effects are likely driven by electrostatic interactions between the positively charged chitosan nanoparticles and negatively charged microbial membranes, resulting in cellular disruption and leakage of intracellular components. These findings emphasize the dual advantage of marine waste valorization and development of potent nanobiomaterials with biomedical and environmental relevance.

Looking forward, the promising characteristics of these CNPs open new avenues for their application in aquaculture wastewater treatment. Aqua industry effluents often contain high levels of nutrients (phosphates, nitrates), organic matter, antibiotics, and microbial contaminants, which can lead to eutrophication and disease outbreaks. Chitosan nanoparticles, owing to their high surface area, cationic nature, and biocompatibility, offer a multifunctional solution by acting as both adsorbents and antimicrobial agents. Future research should focus on evaluating the adsorption efficiency of these nanoparticles for nutrient removal, optimizing their use in real aquaculture effluent systems, and integrating them into filtration or bioremediation platforms. Pilot-scale studies in aquafarms could further validate their impact on improving water quality, enhancing shrimp or fish health, and supporting sustainable aquaculture practices. The incorporation of probiotics or bioactive plant extracts along with CNPs may also enhance their functionality, making them valuable in the development of holistic wastewater treatment systems.

VI. ACKNOWLEDGMENT

The authors gratefully acknowledge the Ministry of Education/Ministry of Human Resource Development, Government of India, for the financial support provided under the Rashtriya Uchchatar Shiksha Abhiyan (RUSA) scheme. This support has been instrumental in facilitating the successful execution of this research work. The authors also extend their appreciation to the institutional RUSA coordination team for their continuous guidance and administrative assistance throughout the project.

REFERENCES

[1] Abdulkarim, A., Isa, M.T., Abdulsalam, S., Muhammad, A.J. and Ameh, A.O. (2013). Extraction and characterisation of chitin and chitosan from mussel shell. Civil and Environmental Research, 3(2), pp.108–114.
[2] Abed, E.H., Al Ameen, N.İ. and Jazaa, L.A. (2017). Extraction of chitosan from Kentish snail exoskeleton shell's, Monacha cantiana (Montagu, 1803) for the pharmaceutical application. Journal of International Environmental Application and Science, 12(2), pp.125–130.
[3] Adekanmi, A.A., Adekanmi, U.T., Adekanmi, A.S., Ahmad, L.K. and Emmanuel, O.O. (2023). Production and characterisation of chitosan from chitin of snail shells by sequential modification process. African Journal of Biotechnology, 22(2), pp.39–53.
[4] Adhikari, H.S. and Yadav, P.N. (2018). Anticancer activity of chitosan, chitosan derivatives, and their mechanism of action. International Journal of Biomaterials, Article ID 2952085.
[5] Akpan, E.I., Gbenebor, O.P. and Adeosun, S.O. (2018). Synthesis and characterisation of chitin from periwinkle (Tympanotonus fusatus) and snail (Lissachatina fulica) shells. International Journal of Biological Macromolecules, 106, pp.1080–1088.
[6] Al Sagheer, F.A., Al-Sughayer, M.A., Muslim, S. and Elsabee, M.Z. (2009). Extraction and characterization of chitin and chitosan from marine sources in Arabian Gulf. Carbohydrate Polymers, 77(2), pp.410–419.
[7] Alabaraoye, E., Achilonu, M. and Hester, R. (2018). Biopolymer (Chitin) from various marine seashell wastes: Isolation and characterization. Journal of Polymers and the Environment, 26, pp.2207–2218.
[8] Anand, M., Kalaivani, R., Maruthupandy, M., Kumaraguru, A. and Suresh, S. (2014). Extraction and characterization of chitosan from marine crab and squilla collected from the Gulf of Mannar Region, South India. Journal of Chitin and Chitosan Science, 2(4), pp.280–287.
[9] Alimi, B.A., Pathania, S., Wilson, J., Duffy, B. and Frias, J.M.C. (2023). Extraction, quantification, characterization, and application in food packaging of chitin and chitosan from mushroom: A review. International Journal of Biological Macromolecules, 237, Article ID 124195.
[10] Anoop, A., Gobinath, T. and Ravichandran, S. (2022). Physicochemical properties and structural characterization of chitosan synthesized from rare spined murex, Murex trapa (Roding, 1798) shell waste. Research Journal of Pharmacy and Technology, 15(12), pp.5729–5735.
[11] Li, H., Huang, W., Qiu, B., Thabet, H.K., Alhashmialameer, D., Huang, M. and Guo, Z. (2022). Effective removal of proteins and polysaccharides from biotreated wastewater by polyaniline composites. Advanced Composites and Hybrid Materials, 5(3), pp.1888–1898.
[12] Ianiro, A., Di Giosia, M., Fermani, S., Samorì, C., Barbalinardo, M., Valle, F., Pellegrini, G., Biscarini, F., Zerbetto, F., Calvaresi, M. and Falini, G. (2014). Customizing properties of β-chitin in squid pen (gladius) by chemical treatments. Marine Drugs, 12(12), pp.5979–5992.
[13] Gbenebor, O.P., Akpan, E.I. and Adeosun, S.O. (2017). Thermal, structural and acetylation behavior of snail and periwinkle shells chitin. Progress in Biomaterials, 6(3), pp.97–111.
[14] Hajji, S., Younes, I., Rinaudo, M., Jellouli, K. and Nasri, M. (2015). Characterization and in vitro evaluation of cytotoxicity, antimicrobial and antioxidant activities of chitosans extracted from three different marine sources. Applied Biochemistry and Biotechnology, 177(1), pp.18–35.
[15] Hazeena, S.H., Hou, C.Y., Zeng, J.H., Li, B.H., Lin, T.C., Liu, C.S., Chang, C.I., Hsieh, S.L. and Shih, M.K. (2022). Extraction optimization and structural characteristics of chitosan from Cuttlefish (S. pharaonis sp.) bone. Materials, 15(22), Article ID 7969.
[16] Vázquez, J.A., Noriega, D., Ramos, P., Valcarcel, J., Novoa-Carballal, R., Pastrana, L., Reis, R.L. and Pérez-Martín, R.I. (2017). Optimization of high purity chitin and chitosan production from Illex argentinus pens by a combination of enzymatic and chemical processes. Carbohydrate Polymers, 174, pp.262–272.
[17] Varma, R., Vasudevan, S., Chelladurai, S. and Narayanasamy, A. (2021). Synthesis and physicochemical characteristics of chitosan extracted from Pinna deltoides. Letters in Applied NanoBioScience, 11, pp.4061–4070.
[18] Singh, A., Benjakul, S. and Prodpran, T. (2019). Ultrasound-assisted extraction of chitosan from squid pen: Molecular characterization and fat binding capacity. Journal of Food Science, 84(2), pp.224–234.
[19] Čadež, V., Šegota, S., Sondi, I., Lyons, D.M., Saha, P., Saha, N. and Sikirić, M.D. (2018). Calcium phosphate and calcium carbonate mineralization of bioinspired hydrogels based on β-chitin isolated from biomineral of the common cuttlefish (Sepia officinalis, L.). Journal of Polymer Research, 25(10), pp.1–12.
[20] Du, Y., Zhao, Y., Dai, S. and Yang, B. (2009). Preparation of water-soluble chitosan from shrimp shell and its antibacterial activity. Innovative Food Science & Emerging Technologies, 10(1), pp.103–107.
[21] El Knidri, H., Belaabed, R., Addaou, A., Laajeb, A. and Lahsini, A. (2018). Extraction, chemical modification and characterization of chitin and chitosan. International Journal of Biological Macromolecules, 120, pp.1181–1189.
[22] George, A. and Roberts, F. (1992). The use of exoskeletons of shrimp (Litopenaeus vanammei) and crab (Ucides cordatus) for the extraction of chitosan and production of nanomembrane. In: Chitin Chemistry, pp.249–267. The Mac Millan Press Ltd.
[23] Gobinath, T., Thamizhselvan, S., Ramakrishnan, A. and Ravichandran, S. (2021). Preparation and characterization of chitosan from Perna viridis (Linnaeus, 1758) shell waste as raw material. Research Journal of Pharmacy and Technology, 14(5), pp.2757–2762.
[24] Jang, M.K., Kong, B.G., Jeong, Y.I., Lee, C.H. and Nah, J.W. (2004). Physicochemical characterization of α-chitin, β-chitin, and γ-chitin separated from natural resources. Journal of Polymer Science Part A: Polymer Chemistry, 42(14), pp.3423–3432.
[25] Gandhi, N., Sree Laxmi, Madhusudhan Reddy, D. and Vijaya, Ch. (2022). Microwave mediated green synthesis of silica nanoparticles, characterization, antimicrobial activity, promising applications in agriculture. World Academic Journal of Engineering Sciences, 9(4), pp.1–15.
[26] Vinusha, B., Gandhi, N. and Vijaya, Ch. (2022). Extraction and characterisation of chitin/chitosan from aquatic waste by using marine fungi. International Journal of Current Science, 12(4), pp.213–231.
[27] Vinusha, B., Gandhi, N. and Vijaya, Ch. (2023). Remediation of thermal power plant effluent with chitosan and chitosan trisodium polyphosphate nanoparticles. International Journal of Enhanced Research in Science, Technology & Engineering, 12(1), pp.97–107.
[28] Vinusha, B., Vidya Sagar Reddy, G., Parvez, Sk. and Vijaya, Ch. (2020). Biological extraction of chitosan from aquatic biowaste – a low cost technology. International Journal of Recent Innovations in Academic Research, 4(6), pp.19–28.
[29] Vidya Sagar Reddy, G. and Vijaya, Ch. (2020). A method of preservation of marine fungi in sterile marine water. Asian Journal of Biological and Life Sciences, 9(1), pp.99–102.

[30] Vinusha, B. and Vijaya, Ch. (2019). Extraction and characterization of chitosan from aquatic biowaste. International Journal for Research in Applied Science and Engineering Technology, 7(4), pp.2217–2220.
[31] Vidya Sagar Reddy, G. and Vijaya, Ch. (2018). Diversity of marine fungi isolated from Nellore coast, Andhra Pradesh, India. Journal for Advanced Research in Applied Sciences, 5(2), pp.853–858.
[32] Vinusha, B., Vidyasagar Reddy, G. and Vijaya, Ch. (2017). Chitosan from shrimp biowaste: potential antibacterial agent. International Journal of Informative & Futuristic Research, 4(5), pp.6398–6403.
[33] Vinusha, B., Vidyasagar Reddy, G. and Vijaya, Ch. (2016). Incidence of vibriosis and antibiogram of isolates from shrimp culture ponds of Nellore coast, A.P. International Journal of Applied and Pure Science and Agriculture, 2(8), pp.55–60.
[34] Vinusha, B., Vidya Sagar Reddy, G. and Vijaya, Ch. (2015). Antibacterial activity of chitosan against Vibrio species isolated from shrimp culture ponds of Nellore coast. Malaya Journal of Biosciences, 2(4), pp.209–213.
[35] Reddy, R.M. and Vijaya, Ch. (2007). Solid state fermentation technique to improve the nutritive value of paddy straw using soil fungi. National Journal of Life Sciences, 4(1), pp.111–118.
[36] Gandhi, N., Shruthi, Y., Sirisha, G. and Anusha, C.R. (2021). Facile and eco-friendly method for synthesis of calcium oxide (CaO) nanoparticles and its potential application in agriculture. The Saudi Journal of Life Sciences, 6(5), pp.89–103.
[37] Gandhi, N., Sirisha, D. and Asthana, S. (2018a). Microwave mediated green synthesis of lead (Pb) nanoparticles and its potential applications. International Journal of Engineering Sciences and Research Technology, 7(1), pp.623–644.
[38] Gandhi, N., Sirisha, D. and Asthana, S. (2018b). Microwave mediated green synthesis of copper nanoparticles using aqueous extract of Piper nigrum seeds and particles characterization. IAETSD Journal for Advance Research in Applied Science, 5(2), pp.859–870.
[39] Gandhi, N., Sirisha, D. and Sharma, V.C. (2014a). Microwave-mediated green synthesis of silver nanoparticles using Ficus elastica leaf extract and application in air pollution controlling studies. International Journal of Engineering Research and Applications, 4(1), pp.1–12.
[40] Gandhi, N., Sirisha, D., Hasheena, M. and Asthana, S. (2014b). Eco-friendly method for synthesis of copper nanoparticles and application for removal of aqueous sulphur dioxide (SO_2) and nitrogen dioxide (NO_2). International Journal of Engineering Research and Technology, 3(11), pp.1253–1262.

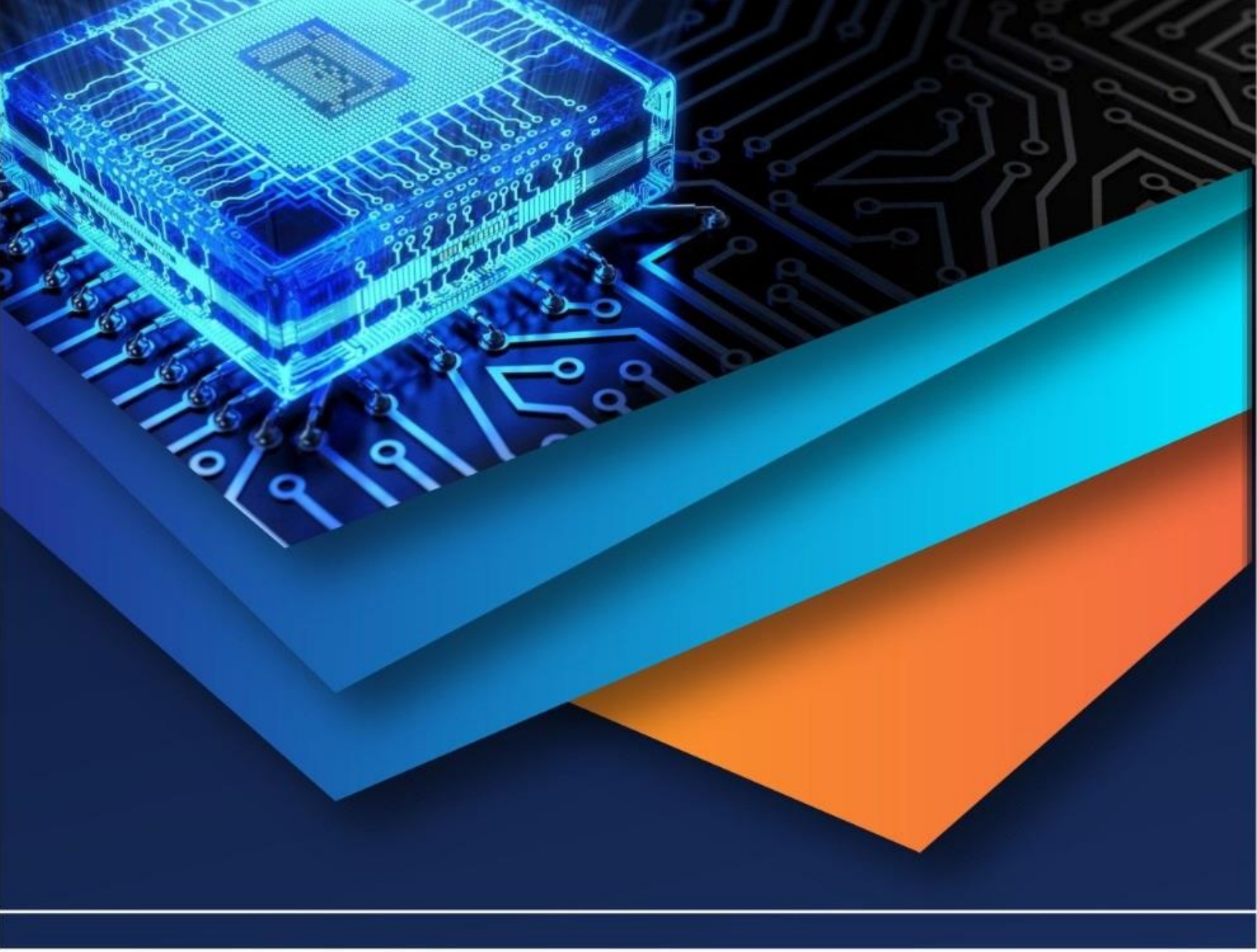

10.22214/IJRASET

45.98

IMPACT FACTOR: 7.129

IMPACT FACTOR: 7.429

INTERNATIONAL JOURNAL FOR RESEARCH

IN APPLIED SCIENCE & ENGINEERING TECHNOLOGY